Journal of Geodesy (2020) 94:40
https://doi.org/10.1007/s00190-019-01327-w

ORIGINAL ARTICLE

Simulation of tracking scenarios to LAGEOS and Etalon satellites

F. Andritsch[1] · A. Grahsl[1] · R. Dach[1] · T. Schildknecht[1] · A. Jäggi[1]

Received: 18 September 2018 / Accepted: 5 December 2019

Abstract
The International Laser Ranging Service (ILRS) provides weekly solutions for coordinates of Satellite Laser Ranging (SLR) stations coordinates, geocenter coordinates, as well as Earth rotation parameters with a daily resolution. The ILRS standard solution is an important contribution to the International Terrestrial Reference Frame (ITRF). As of today, it is derived from SLR observations to the pairs of LAGEOS and Etalon satellites exclusively. In this paper, the effect of altering the tracking strategy for the LAGEOS and Etalon satellites on the weekly ILRS standard solution is studied. This is done by simulating various tracking scenarios and by comparing the parameters of the solutions for each scenario. In particular, the focus lies on redistributing observation time between the LAGEOS and Etalon satellites as a possible optimization for the tracking scheduling. By this, the current tracking capability of each station is taken into account with no change of the overall tracking activity to LAGEOS and Etalon. It is shown that the quality of the solution for the ITRF-relevant parameters is not significantly degraded when reducing the number of observations to LAGEOS by up to 20% with respect to the number of available normal points in 2016. The vacant tracking capability obtained from the reduction of LAGEOS observations may be used to increase the number of measurements to Etalon by a factor of three. This leads to nearly 10% improvement of the recovery of Earth rotation parameters within the combined LAGEOS–Etalon solution. With our study, we contribute to the ongoing discussions regarding tracking strategies for SLR stations within the ILRS. In particular, the stations could adjust their individual tracking priorities according to these results in the future without major investments or the need for new infrastructure.

Keywords Satellite Laser Ranging · SLR simulation · SLR tracking optimization · LAGEOS · Etalon · Earth rotation parameters

1 Introduction

The International Laser Ranging Service (ILRS, Pearlman et al. 2002) standard solution provides an important contribution to the International Terrestrial Reference Frame (ITRF, Altamimi et al. 2016). It delivers weekly estimates for Satellite Laser Ranging (SLR) station coordinates, geocenter coordinates, as well as Earth rotation parameters (ERPs) with a daily resolution. They are obtained exclusively from SLR observations to the pairs of LAGEOS and Etalon satellites (an extension to include LARES is currently under consideration).

About 50 inhomogeneously distributed SLR tracking stations contribute to the ILRS activities. Not all of them are operational at the moment. The majority of stations are located on the Northern hemisphere, with a particularly high density of stations in Europe.

Figure 1 shows the stations that were actively tracking in 2016. The figure also shows the considerable inequality of the productivity of each station in terms of number of normal points, (Sinclair 1997, NPs, binned full-rate observation data) to the two LAGEOS satellites. The size of the circles is proportional to the total number of NPs collected and the different colors group the station into groups of similar productivity levels. While the Australian station Yarragadee was able to submit more than 22,000 NPs to LAGEOS in 2016, twelve European stations with their higher spatial density were able to provide roughly the same number of NPs as Yarragadee. Besides that, about half of the stations submitted less than 2500 NPs in the year 2016.

In 2016, the 38 active stations collected on average a total of nearly 130,000 NPs per month to all target satellites of the ILRS. Typically 13,000 or 10% of those NPs are mea-

✉ F. Andritsch
florian.andritsch@aiub.unibe.ch

R. Dach
rolf.dach@aiub.unibe.ch

[1] Astronomisches Institut, Universität Bern, Bern, Switzerland

Published online: 16 March 2020

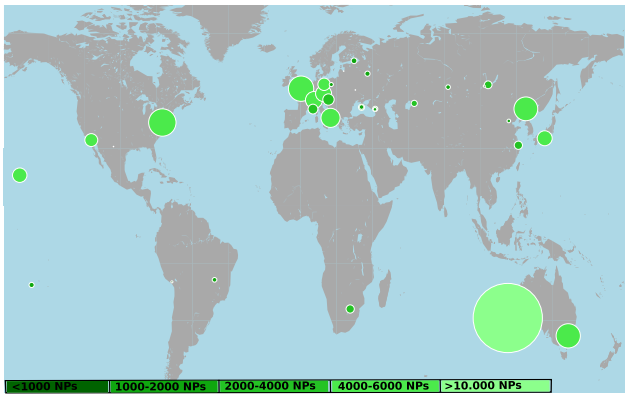

Fig. 1 The stations of the ILRS network and their number of observations to LAGEOS in 2016

surements to the two LAGEOS satellites (out of currently approximately 80 targets), whereas there were only about 1200 observations to the two Etalon satellites in the same period of time. This implies that Etalon NPs account for only about 10% of all observations used for the weekly ILRS standard solution. In the ILRS imbalances between observations to other SLR targets, e.g., Stella, Starlette, GNSS satellites, etc., exist when compared to LAGEOS, with a large number of total NPs provided to these two satellites. This raises the question whether this high volume of observations to only two LAGEOS satellites is really needed, or whether the tracking capacity of the SLR stations could also be used for other targets without significantly degrading the weekly ILRS standard solution.

To study a possible optimization of the weekly solution in the context of a realistic simulation environment, it is assumed that the total number of observations can not simply be increased without essential changes to the infrastructure or operations of the stations. We therefore focus on constructing different tracking scenarios by redistributing NPs from specific satellites to others.

Based on this redistribution idea, first the number of LAGEOS NPs is reduced up to a point where the quality of the solution starts to suffer. Then the tracking capacity that became available is used to increase the Etalon NPs by the same amount. Therefore, the total number of NPs produced for the weekly ILRS solution by the network does not change. This ensures that none of the other supported missions receive less tracking effort. Stations could be asked to follow such an altered prioritization by adjusting the ILRS priority list. Most importantly, this can be done without altering the overall tracking activity per station or investments on station level.

In all subsequent experiments the real NPs were replaced by simulated NPs to allow a meaningful comparison between the different tracking scenarios. Any potential coordination of the tracking activities between the stations is not considered in this study, but supposedly this might have the potential for further optimizations of the tracking scheduling. It would already require, however, additional infrastructure and developments in order to exchange the information about successful NP generation and the processing of this information at the stations.

Numerous other simulation studies exist to examine possible improvements of the weekly ILRS standard solution. The basic concepts studied were, e.g., an increase in overall station observation output and an expansion of the SLR station network by adding new stations. The effect of these possible improvements on the parameters of the weekly ILRS solution, station coordinates in particular, was studied, e.g., by Pavlis and Kuzmicz-Cieslak (2008) and Kehm et al. (2018). They showed that both a higher number of observations per station as well as more SLR stations reduce the scatter of the network translation parameters, improve the scale and result in better ERPs. Additionally, simulation experiments examining the effect of expanding the network have been conducted by Otsubo et al. (2016). These simulations also showed that additional stations would be beneficial for the parameters of the weekly ILRS standard solution. However, the realization of these simulation results requires additional infrastructure and resources for the operation. This legitimates the question whether the currently available tracking capacity of the existing ILRS network is optimally used.

The operational version of the Bernese GNSS Software (Dach et al. 2015) was used for the simulation of the NPs, the processing of the simulated data, and the comparison of the weekly solutions.

In the following parts of this paper, the simulation strategy is introduced in Sect. 2 and the effect of the simulated noise on the solutions is evaluated in Sect. 3. In Sect. 4, different solutions with a reduced number of observations to LAGEOS are computed and compared. Eventually, in Sect. 5 the number of Etalon NPs will be increased and the effects on the parameters of the solution are studied. Furthermore, in Sect. 6 the impact of a system specific range bias to the Etalon satellites on the same parameters is analyzed. Section 7 finalizes the paper with a summary and conclusions.

2 Simulation of SLR observations

The simulation of the SLR observations used for all further experiments is based on the distance derived from the geometry between the satellite and the station at a given epoch. This distance is obtained using a set of weekly SLR station coordinates and satellite orbits from a standard SLR analysis computed at the Astronomical Institute of the University of Bern (AIUB) on a regular basis in accordance with the ILRS solution (Thaller et al. 2011).

The simulation includes the standard corrections for relativistic effects and center of mass offsets that are consistently reapplied during the data processing. All time and range biases are assumed to be zero at this point for the simulation.

A pseudorandom noise is added to the simulated exact distances to resemble the measurement uncertainties. It is based on a white noise function that is scaled with the bin-RMS as reported in the observation files given in the Consolidated Laser Ranging Data (CRD) Format (Ricklefs and Moore 2009). This operation is done in order to represent the noise characteristics of real measurements for each specific pair of station and satellite separately. The goal was to achieve residuals that are comparable in extent to the residuals of the measured NPs.

With a mean value μ_{ij} and the standard deviation σ_{ij} derived from the given two-way bin-RMS of all the NPs for each pair of station i and satellite j, the polar method described in Marsaglia and Bray (1964) is used to get a series of standard normally distributed random numbers with mean 0 and standard deviation 1

$$x = u_1 * \sqrt{\frac{-2\ln(u_1^2 + u_2^2)}{u_1^2 + u_2^2}}$$

from two uniformly distributed series of random numbers u_1, u_2 based on an initial seed.

These random numbers are generated with the RANLUX algorithm (James 1994). Other random number generators including a mersenne twister (Matsumoto and Nishimura 1998; Nishimura 2000), and a linear congruential generator (Knuth 1997), were also evaluated. RANLUX was chosen for being faster than the Mersenne twister and superior to a linear congruential generator in terms of periodicity.

Using x, a series z of normally distributed random numbers with the mean value μ_{ij} and standard deviation σ_{ij} can be obtained by

$$z = \sigma_{ij} * x + \mu_{ij}. \quad (1)$$

Each element of this series is assigned to the noise of a potential measurement from a station to a satellite, independent of whether this particular observation is selected in the simulation scenario or not. In case a certain observation is simulated, the pseudorandom noise is added to the exact distance computed from the observation geometry at the given epoch. The exact value is half of the parameter derived from the two-way bin-RMS. One of the advantages of this approach is the possibility to reproduce the same noise for a certain observation at a given epoch, even if the remaining observation schedule is changed. This allows a direct comparison of different observation scenarios where coinciding observations retain the same noise level. In the case where a different set of independent noise parameters is required, the random number generator can be initialized with a different seed. Furthermore, with this technique numbers of the random series of random numbers are picked only sporadically, making the simulated noise insusceptible to potential systematics of the random number generator.

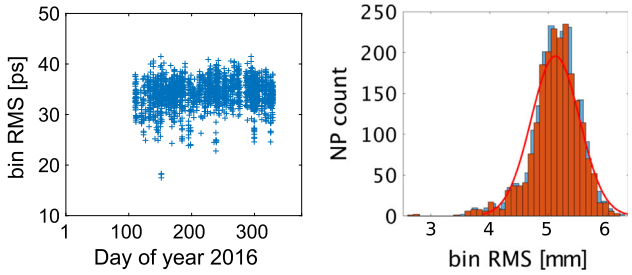

Fig. 2 Left: reported two-way bin-RMS of NPs taken from the CRD files. Right: normal distribution (red line) modeling the noise of the simulated observations (orange) of station 7839 (Graz) to LAGEOS 2 based on the distribution of the bin-RMS of real NPs (light blue). The same procedure was conducted for each pair of station and satellite

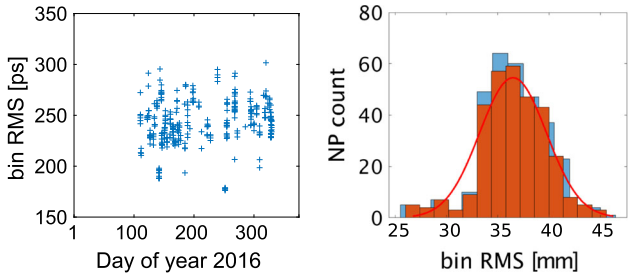

Fig. 3 Left: reported two-way bin-RMS of NPs taken from the CRD files. Right: normal distribution (red line) modeling the noise of the simulated observations (orange) of station 7839 (Graz) to Etalon 2 based on the distribution of the bin-RMS of real NPs (light blue). The same procedure was conducted for each pair of station and satellite

Using the reported two-way bin-RMS to rescale the simulation noise results in modeling a different noise for each station observing LAGEOS, resembling station specific differences in measurement accuracy. In addition, a different simulated noise for the Etalon satellites compared to the LAGEOS satellites is obtained, taking into account different system specific accuracies for each station. Notably, the noise of Etalon observations is about five times higher for most stations due to a number of possible factors. The target depth is larger for the Etalon satellites compared to LAGEOS. The signal drop-off at larger distances of roughly 19,000 km compared to 6000 km in the case of LAGEOS is another contributing factor.

One distribution per station and satellite is modeled for the entire year. The result of one noise simulation run for LAGEOS2 and Etalon2 observations taken in 2016 by the SLR station in Graz (7839) is shown as an example in Figs. 2 and 3, respectively. It can be observed that the modeled

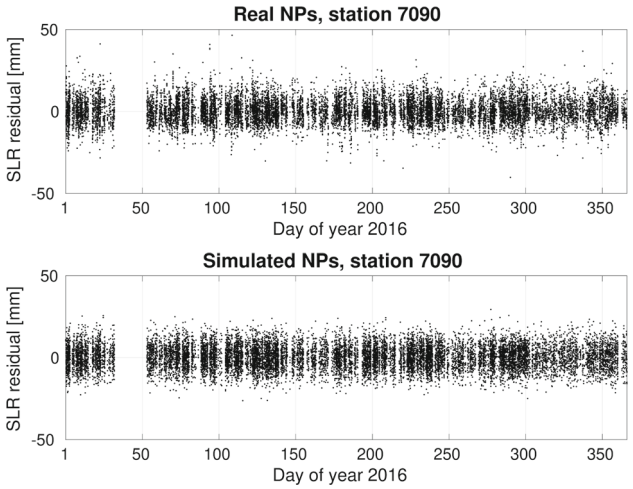

Fig. 4 Comparison of residuals from real observations of station 7090 (Yarragadee, Australia) to both LAGEOS satellites (top) and the residuals of simulated NPs at the equivalent epochs (bottom)

Gaussian distribution reasonably approximates the distribution of reported bin-RMS values by construction. The slight deviation from a perfectly symmetrical Gaussian distribution originates from the limited number of simulated noise values, especially for Etalon, and the bin size. In addition for satellites with a low total number of NPs in a given year, outliers have a larger impact on the distribution.

Figure 4 shows the real and simulated residuals to LAGEOS satellites for the station 7090 (Yarragadee, Australia). The real residuals were computed by the standard method of comparing the real observations with a computed orbit. The simulated residuals were computed using simulated observations instead of real ones, but compared to the same orbits. It is important to note that the reference orbits were used as input for the simulation. The result is a very similar residual distribution for both sets of NPs.

The residuals of the simulated NPs have a minimum value of -26.3 mm and a maximum of $+29.4$ mm. About 98% of the real NPs have residuals within this range, resulting in only a small number of outliers of NPs with larger residuals in the real measurements than in the simulations. This is expected, because real measurements are prone to technical issues resulting in higher measurement errors from time to time. The 25% and 75% quartiles for the real NPs are -4.2 mm and $+4.6$ mm, respectively, and compare well with the corresponding quartiles of the simulated observations of -4.6 mm and $+5.3$ mm. For other stations, the residuals of the simulated observations correspond to the ones of the real NPs on a comparable level as for the station 7090.

From this, it can be concluded that the chosen simulation strategy results in a reasonable residual characteristic which is well suited for realistic experiments. Seasonal variations in the residuals of real NPs are supposed to originate from modeling deficiencies and are, therefore, not modeled in the simulated noise.

All simulated tracking scenarios presented in the following sections take the actual station performance into account. This implies that for each station only the total number of actually submitted NPs was simulated. When simulating different scenarios with additional NPs, satellite visibilities were taken into account. Also, a station was only declared as available at epochs when it indeed submitted NPs in 2016. This resembles the situation within the ILRS network in a realistic way with a different level of productivity for each station.

We generated a variety of tracking scenarios by starting with the case of the observation scenario containing the NPs that have been provided by the stations in 2016. This is referred to as *reference scenario* throughout this paper. When in later scenarios, a certain amount of LAGEOS NPs are redistributed to Etalon observations, only epochs during which LAGEOS was observed and Etalon was visible for a given station at the same time were considered for a swap of the observation target.

3 Comparing the solutions from real observations to the simulation for the reference scenario

Before analyzing different tracking scenarios, the consistency of the solution of station coordinates, ERPs, and satellite orbits in the case of a one-to-one replacement of real NPs with simulated observations was assessed. This first step ensures that all corrections are applied consistently in the simulation and the processing of the simulated NPs.

Following the ILRS standard procedure, a solution using the simulated observations was determined for each week of 2016. The resulting SLR station coordinates are compared to the positions introduced in the simulation using a seven parameter Helmert transformation (three translation parameters, three rotation parameters, and one scale parameter).

To establish the effect of the simulation noise on the solution, multiple sets of NPs with varying initial seeds for the random number generator are created and it is checked how the various parameters are affected. This gives a threshold to distinguish between purely noise related effects in the solution and geometric effects due to the distribution and availability of NPs in different scenarios.

Figure 5 displays the average RMS of the Helmert transformation and the spread for multiple sets of simulated observations using ten different initial seeds. The average RMS of the Helmert transformation during the year is 3.4 mm and the solutions for 1 day typically lie within less than 1 mm. This means that the main part of the variation between the weeks in Fig. 5 is the result of the different spatial and tempo-

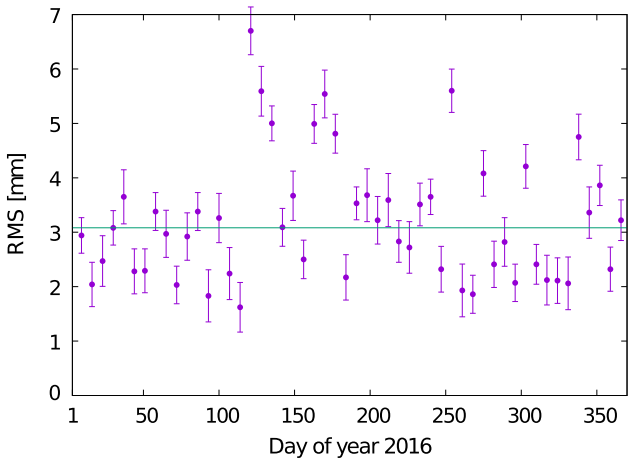

Fig. 5 RMS of the Helmert transformation between the weekly solution of station coordinates used for the simulation and estimates derived from simulated NPs. Displayed is the range of RMS values given by 10 runs with different initial seeds for the random noise generation (purple dots with bars) and the median RMS (green line)

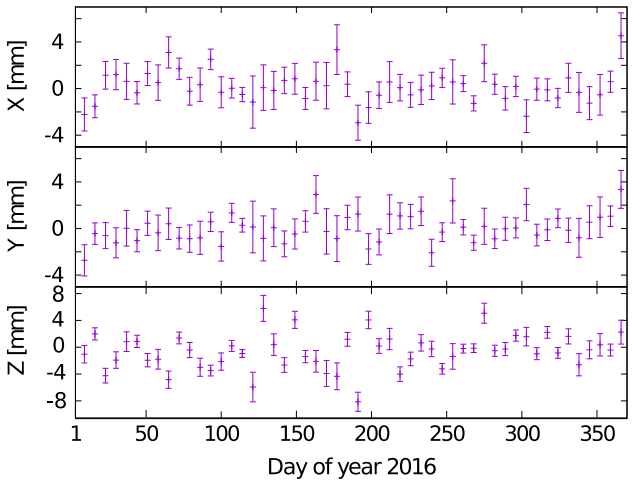

Fig. 6 Translation parameters and formal errors of the Helmert transformation between the weekly solution of station coordinates used for the simulation and the solution derived from the simulated NPs

ral availability of NPs from week to week. The median RMS is 3.1 mm and was chosen to serve as a threshold parameter for the comparison of the quality of alternative tracking scenarios.

Figure 6 displays the three translation parameters (in X, Y and Z direction) and formal errors of the Helmert transformation between the station coordinates used for the simulation and the solution based on the simulated NPs. It shows that the mean translation parameters are in the range of within ± 3 mm for the X and Y components and may reach up to -8 mm and $+6$ mm in weeks with the largest differences for the Z component.

The average over all weeks is smaller than 0.5 mm for each component. The formal error of the translation parameters is consistent with the RMS of the Helmert transformation by construction; weekly solutions with a higher RMS also show larger formal errors of the translation parameters.

Comparing the translation parameters of the Helmert transformation for solutions derived from simulated NPs using different initial seeds results in solutions that lie within roughly 0.5 mm of each other (not shown). Changing the seed of the random number generator, therefore, has again a smaller effect on the translation parameters than the geometric properties of the weekly changing distribution of NPs themselves.

In analogy to the translation parameters discussed above, the three rotation parameters of the Helmert transformation between the station coordinates used for the simulation and the processing results using the simulated NPs were analyzed. The resulting values are in the range of ± 1.5 mas in the X and Y components. In the Z component, while there is a single outlier of -3 mas in a week with one of the lowest number of observing stations and only very little contribution from European stations. All other values are in the same range of ± 1.5 mas. The mean values of each of the rotation parameters are less than 0.2 mas, which is equivalent to approximately 6 mm at the surface of the Earth. The weekly variations and formal errors show the same deviations as the translation parameters above. Varying the initial seed accounts for differences of the weekly solutions within 0.4 mas in all three components.

Furthermore, the values of the scale of the Helmert transformation are ranging from -0.4 to 0.2 ppb with a mean value of 0.08 ppb. This corresponds to only 0.5 mm at the Earth's surface. The effect of different seeds is on the level of ± 0.05 ppb. This proves to be smaller than these values in accordance with the translation and rotation parameters and the RMS of the Helmert transformation.

In summary, from these seven parameters of the Helmert transformation it can be concluded that overall no significant change of the station geometry is introduced by using the NPs from our simulation for the determination of the coordinates. Furthermore, the effect of different initializations of the random noise function in the simulation is smaller than the typical variation from week to week.

This variation between the different weeks originates mainly from the highly fluctuating number of available NPs and their spatial distribution. For LAGEOS, typically 17 to 33 stations provide NPs for a weekly solution, while for Etalon, usually only half of this number of stations contribute observations.

Figure 7 shows the weekly available NPs for the two regions contributing the majority of NPs; while the station Yarragadee (7090) delivers a relatively constant number of NPs per week throughout the year, other stations located, for example in Europe, are subject to considerably less stable

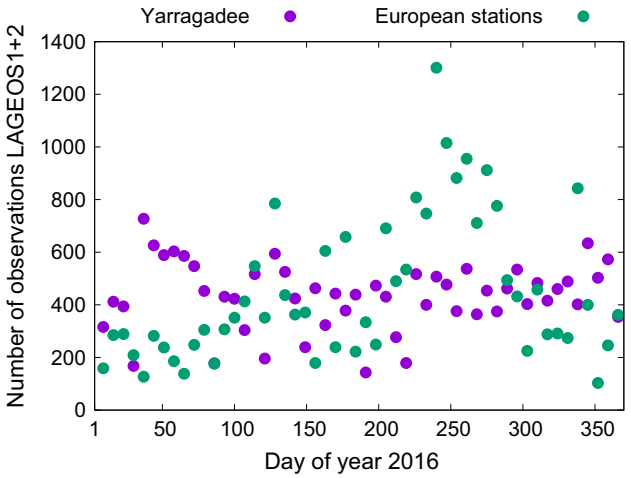

Fig. 7 Comparison of available NPs to LAGEOS1 and LAGEOS2 from station 7090 (Yarragadee) and the six most productive stations in Europe (7810 Zimmerwald, 7839 Graz, 7840 Herstmonceux, 7841 Potsdam, 7941 Matera, 8834 Wettzell)

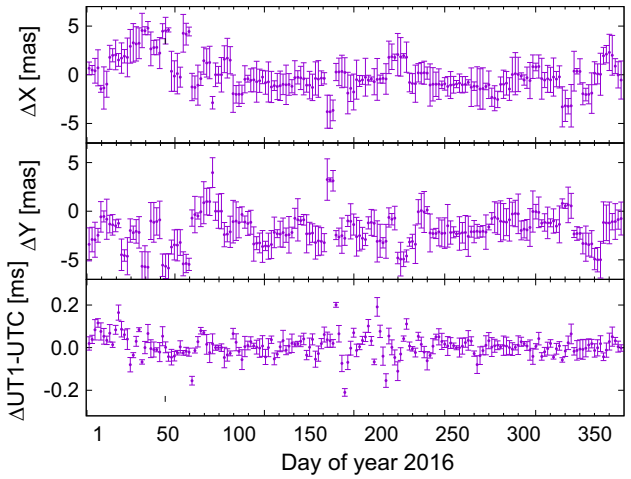

Fig. 8 Differences of ERPs used for the simulation and ERPs derived form simulated NPs. The error bars display the formal error of the solution

weather conditions and are not able to maintain the same level of observations each week.

In weeks with fewer observations and less stations worldwide being able to observe at all, there is a larger uncertainty in the estimated coordinates and thus also in the Helmert parameters. The number of stations also directly impacts the spatial distribution of available observations. This can be seen for example in the varying size of the error bars in Fig. 6. Also, the fewer observations are simulated for a station, the more the simulation noise suffers from the selection bias and does not perfectly cover the Gaussian distribution for the corresponding station as described in Fig. 2.

Furthermore, a time series of geocenter coordinates was estimated in a standard solution from real NPs to LAGEOS and Etalon collected in 2016. We use this as a reference against which to compare the solution from simulated NPs. The median of the difference is 5.6 mm in X, 1.5 mm in Y, and 0.2 mm in Z direction. The scatter of the differences has 25% and 75% quartiles of -28.6 mm and $+20.2$ mm in the X, -24.4 mm and $+22.4$ mm in the Y, and -26.6 mm and $+23.3$ mm in the Z component. Different seeds result in geocenter coordinates within 5 mm of each other in all components, meaning that the observation noise contributes only 20% to the geocenter coordinates estimation uncertainty. The remaining larger part and therefore much more important effect is the distribution of stations and observations.

To analyze the quality of the estimated ERPs, they are compared to the ERPs used for the simulation. The differences between these sets of ERPs are shown in Fig. 8 for every 48 h. We can see that X- and Y-pole differences between the solution from simulated observations and the ERPs used for the simulation are in the range of ± 5 mas. The difference in the length of day (LOD) parameter is ranging within ± 0.2 ms. The larger differences in the first 50 days of 2016 result from the lower number of observations provided by the stations in the Northern hemisphere during winter times. The formal errors are on the same order of magnitude for each week. Typically, however, weeks with larger differences also have a slightly bigger formal error.

Apart from the station coordinates and ERPs, 7-day orbits for both LAGEOS and Etalon satellites are estimated. When comparing the resulting orbits from simulated data with the orbits used in the simulation they agree by 100 mm in all components of an Earth-fixed coordinate frame for LAGEOS1. The RMS of the differences is 28 mm in average over all three components for LAGEOS1 (see Fig. 9). The orbits for Etalon1 agree on a level of 300 mm maximum difference in all components of an Earth-fixed coordinate frame and average RMS of 43 mm (see Fig. 10). Similar values are obtained for LAGEOS2 and Etalon2, respectively. As expected, due to a smaller number of observations paired with a five times larger observation noise, the uncertainties for Etalon are larger than for the better observed LAGEOS.

There are certain weeks where differences are twice as big as for the majority of other weeks caused by the changing availability of observations per station and geographic region (Fig. 7). The larger differences from day 100 to 107, e.g., show that for this week's solution there are both few observations available from the six most productive stations in Europe, and also few from the Southern hemisphere station 7090 Yarragadee in Australia. In the period from day 44 to 72, Yarragadee was providing the largest number of NPs (around 750) and Europe was still contributing with around 250 NPs, which leads to among the smallest orbit differences for this year of about ± 20 mm for LAGEOS1 and ± 50 mm for Etalon1. When either Yarragadee provides less than average NPs or both Yarragadee and the European output is below average, the orbit differences increase. Sim-

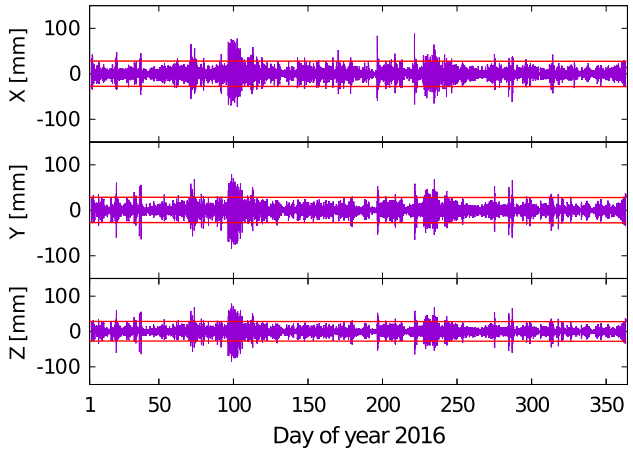

Fig. 9 Differences in LAGEOS1 orbits used for the simulation and estimated from simulated NPs. The red line is the average RMS of the differences

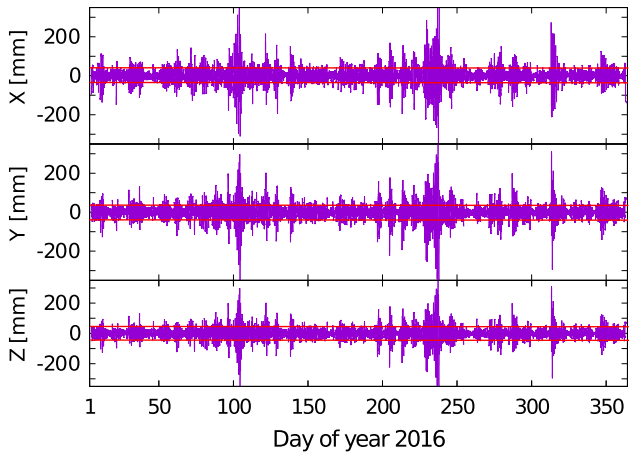

Fig. 10 Differences in Etalon1 orbits used for the simulation and estimated from simulated NPs. The red line is the average RMS of the differences

ilarly, the days around day 240 with larger differences show an imbalance in the available NPs between the hemispheres. In particular, station 7090 performs comparably lower than average and the European stations are below average as well, showing that both, a low number of NPs or a larger imbalance between available NPs observed in the Northern or Southern hemisphere, lead to larger differences in the estimated orbits.

In conclusion, the results presented in this section show that the contribution of the noise to the weekly variation is smaller than the geometry of the available NPs. The variations are summarized in Table 1 and define the variation threshold combined with contribution of the noise to the solution resulting from our simulated observations. In the following sections, other tracking scenarios will be compared to the values discussed in this section. If the parameters of a certain scenario exceed the boundaries for the variations, it is considered to be worse than the reference scenario.

Table 1 Summary of parameter thresholds determined by the simulation

Parameter	Range	Assumed threshold
RMS coordinates	1.5 to 6.8 mm	3.1 mm
Translation parameters	± 3 mm	2.5 mm (*X*, *Y*)
	− 8 to + 6 mm	2.5 mm (*Z*)
Rotation parameters	± 1.5 mas	1 mas
Scale	− 0.4 to + 0.2 ppb	0.15 ppb
Geocenter coordinates	− 28 to + 24 mm	9 mm (*X*, *Y*, *Z*)
ERPs	± 10 mas	3 mas (*X*, *Y*)
	± 1 ms	0.9 ms (LOD)
LAGEOS orbit differences	± 10 mm	38 mm
Etalon orbit differences	± 300 mm	43 mm

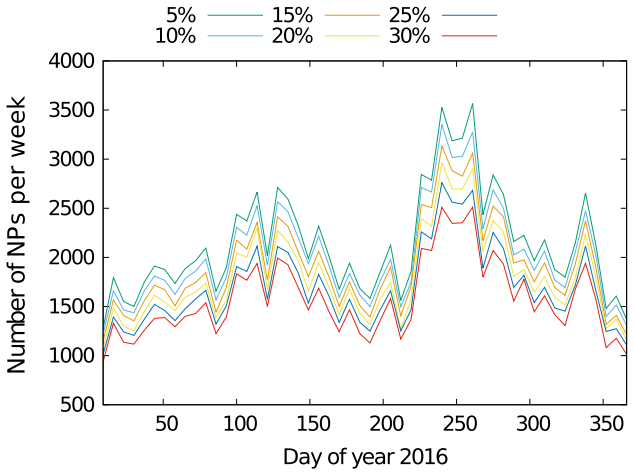

Fig. 11 Number of NPs for LAGEOS for the different scenarios

4 Reduction of LAGEOS observations

Starting from the real observation activities of all stations in 2016, six reduced LAGEOS tracking scenarios were defined. Each NP was replaced by a synthetic observation and the number of NPs was reduced step by step by up to 30% (see Fig. 11).

Single observations were omitted randomly with equal probabilities for all stations. This corresponds to a likely behavior of the SLR stations if the general priority list is adapted accordingly by the ILRS.

Simulated observations are used instead of simply reducing the real NPs for two main reasons. It allows for a comparison of solutions using different seeds for the simulation noise, and also enables a direct comparison to solutions derived from tracking scenarios with more NPs than actually observed, as it will be discussed in Sect. 5.

The station and geocenter coordinates, ERPs, and orbits for all the scenarios with reduced tracking of the LAGEOS satellites were compared to the reference solution derived

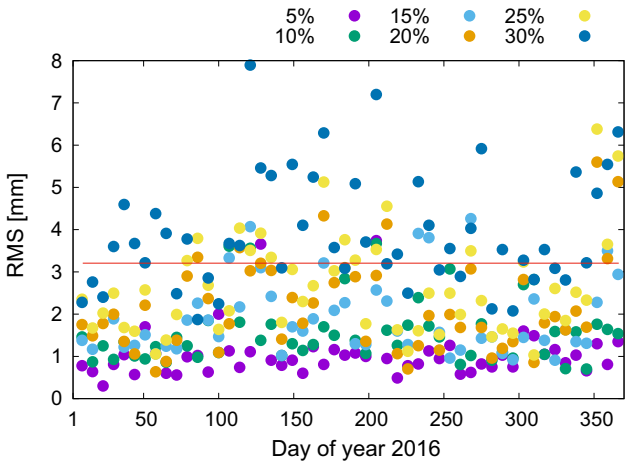

Fig. 12 RMS of the Helmert transformation between resulting station coordinates and the solution derived from simulated NPs without any reduction. The red line highlights the threshold established in Table 1

from simulated NPs without any reduction. This establishes a controlled environment where the same corrections are applied in the simulation and the processing of the synthetic observations.

The effect of the geometric distribution of available observations is visible in Table 1. This gives a quality baseline and can be taken as a reference to what extent a reduction is acceptable. If the values of a scenario remain within the effect of the geometry, then the overall quality is assumed not to be significantly different from the reference scenario (scenario with no reduction).

First, the estimated station coordinates for all scenarios are compared to the reference solution without reduction (in Fig. 12). With each 5% step of reduction, the RMS of the Helmert transformation between each scenario and the reference solution increases by 0.4–0.5 mm. At the same time the formal errors of the station coordinates increase slightly from less than 8% for scenarios up to 15% reduction. Furthermore, the formal errors increase to 13% for 20% reduction and to almost 20% for the case of 30% reduction of LAGEOS observations.

We assumed that the number of stations contributing to the solution was not altered by this reduction. Lowering the number of LAGEOS NPs of a given station up to the levels considered in this study should not lead to any station being excluded in the processing.

The scenarios in which the measurements were reduced by up to 20% show an RMS for the Helmert parameters that are below the variation of RMS value in the coordinates when varying the seed of the simulation noise, as established in the previous section (Fig. 5 and Table 1).

In the 5%, 10% and 15% reduction scenario only single weekly RMS values of the Helmert transformation are slightly above the 3.1 mm threshold with values of 3.2–4.15 mm maximum.

The vast majority of weekly coordinate solutions remain far below the threshold. In the 20% reduction case, 6 out of 52 solutions have an RMS above 3.1 mm while the rest of the weeks remain below that level.

The scenario with 25% reduction contains 15 of 52, which is almost 30% of the weekly solutions with RMS above 3.1 mm and 32 out of the 52, or 60% of the weeks are above the average RMS value for the scenario with 30% reduction.

The translation and rotation parameters of the Helmert transformation of the station coordinates for all different reduction scenarios were compared to the noise threshold (Table 1). When only considering the reduction scenarios up to 20%, the translation parameters range between ± 2 mm for all three components, which is well within the noise floor of ± 3 mm in X and Y as well as -8 mm and $+6$ mm in the Z component.

In the 25% and 30% reduction scenarios, 10 and 34, out of 52 solutions exceed these limits. The largest values belong to solutions of the 30% reduction scenario.

Similar to the translation parameters, the components of the rotation parameters range between ± 0.5 mas in the X and Y component and between -1 mas and 0.5 mas in the Z component for the cases of 5–20% reduction, remaining within the noise threshold of $\pm$ 1.5mas.

The 25% and 30% reduction results in rotation parameters in the range of $\pm$ 1.5 mas in the X and Y component and ± 2 mas in the Z component with again 11 and 29 out of 52 values exceeding the limits for the 25% and 30% reduction scenarios successively. Compared to the rotation parameters established in Table 1, these values have a significantly increased scatter for reduction scenarios higher than 20%.

The same applies for the scale component of the Helmert transformation.

When comparing the geocenter coordinates of the different scenarios with the same reference geocenter used in Sect. 3, they lie within 20–30 mm difference, with only few outliers larger than that. However, it can be observed that the scatter of the differences to the reference geocenter coordinates increases with a reduction of observations.

A box plot of the differences (Fig. 13) clearly shows how the solutions for the geocenter get worse with high reductions of LAGEOS observations. While the maximum differences remain the same in good approximation, the scatter of the coordinate differences remains almost at the same level of roughly -10 mm to $+10$ mm for the 25% and 75% quartile up to 20% reduction in all components.

For higher reductions, the scatter increases in the 25% reduction case to -15 mm for the 25% and $+11$ mm for the 75% quartile, and even larger in all components for the 30% reduction case The median remains stable below 10 mm for all three components.

The quality of ERP recovery varies between the weekly solutions (Fig. 14). The variation between the weekly solu-

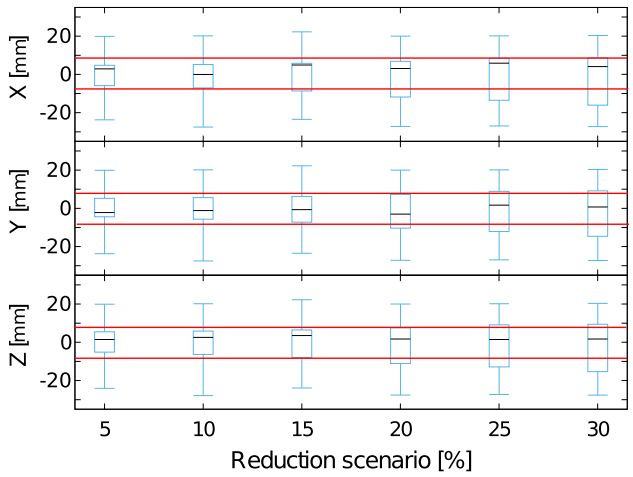

Fig. 13 Box plot of geocenter differences of the reduced tracking with respect to the original tracking scenarios. The red line highlights the threshold established in Table 1

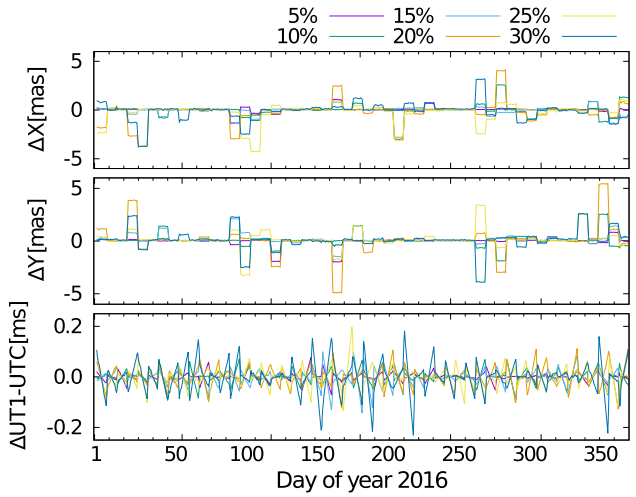

Fig. 14 Differences between ERPs of the simulated reduction scenarios and the solution derived from simulated NPs without any reduction

tions is a result of the varying station availability. In weeks where already larger differences and formal errors were seen in Fig. 8, also larger differences with higher uncertainties can be seen in the reduction scenarios. Overall, the difference between the scenarios up to 20% reduction is not significant when compared to the noise threshold of the simulation (compare Table 1).

The results in this section indicate that it is feasible to reduce the number of LAGEOS NPs by up to 20% while remaining within the boundaries as established in Table 1.

In the processing of the reduction scenarios, a possible implementation of such a reduction via adjusting the ILRS priority list and not expanding the stations tracking capabilities was considered. The overall coverage of stations providing observations should be distributed as well as possible over the network.

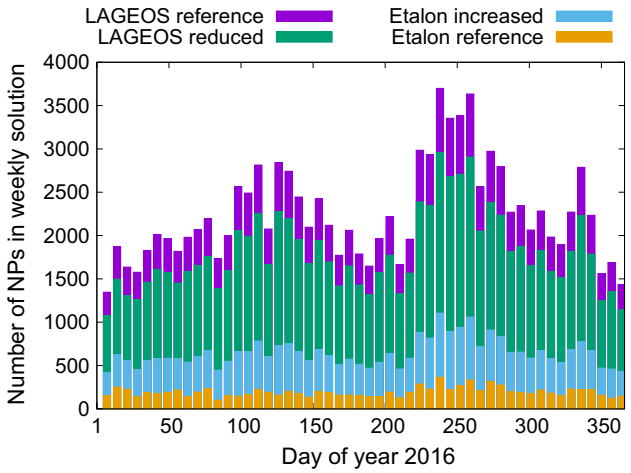

Fig. 15 Number and distribution of LAGEOS and Etalon observations in the reference case and with increased priority for Etalon

5 Increasing the number of Etalon observations

As shown in the previous section, the simulated scenarios suggest that it is possible to have 20% fewer LAGEOS observations in the weekly solutions without degrading the quality of the results significantly.

This justifies experimenting with reducing the number of LAGEOS NPs in favor of increasing the number of Etalon NPs to the same extent in the combined solution in order to not reduce the number of measurements contributing to the ITRF-relevant solutions. This increases the number of Etalon observations from 10 to 30% of the NPs compared to LAGEOS in the weekly solutions. The total number of NPs provided by each station for the ILRS standard solution hereby remains the same. This means that also the degree of freedom in the least squares analysis is preserved because the number of estimated parameters and available observations is not changed. Therefore, the results for the parameters can be compared directly as they were estimated from a constant amount of observations. However, the amount of Etalon NPs with a higher noise level than LAGEOS NPs is increased.

Additionally in this scenario all stations are delivering NPs to all four satellites since 20% of all NPs to LAGEOS were replaced with NPs to Etalon for every active station. This also significantly improves the coverage of Etalon observations within the station network.

We study the effect of having almost three times as many Etalon NPs in the processing (Fig. 15). Although these NPs have a higher noise (up to 5 times depending on the station) than LAGEOS NPs, we want to study whether the standard solution can benefit from the different orbital geometry of Etalon if there are three times as many observations to Etalon.

With an increased number of Etalon observations, the a posteriori RMS of unit weight is on average, approximately

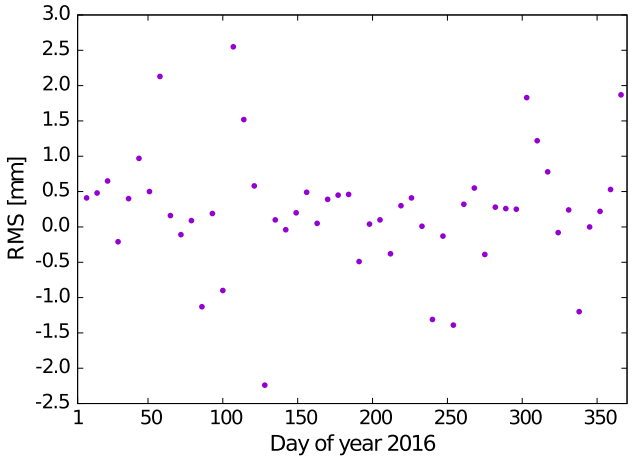

Fig. 16 Differences of Helmert transformation RMS values between the reference solution and the scenario with an increased amount of Etalon measurements

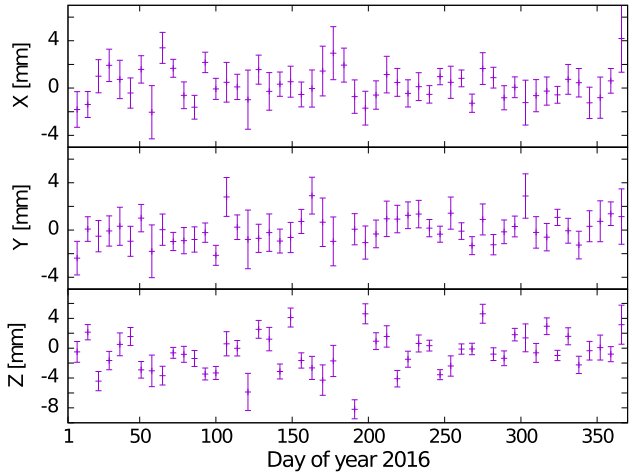

Fig. 17 Translation parameters of the Helmert transformation of station coordinates derived from the increased Etalon scenario and the original scenario using simulated NPs

5% higher than in the reference solution with unaltered numbers of observations. This is expected because in this case, 20% of the observations are replaced with ones featuring a up to 5 times higher noise.

As in the previous section, the station coordinates are checked via the parameters of the Helmert transformation between the station coordinates used for the simulation and the results of the scenario with additional Etalon observations. The difference between the RMS value of the Helmert transformation for the station coordinates of the simulated reference scenario and this scenario is at the mean level of 0.5 mm (Fig. 16), i.e., well within the threshold established in Table 1 in Sect. 3. This implies that the overall RMS does not change significantly by replacing 20% of LAGEOS NPs with Etalon NPs and confirms that the obtained station coordinates are still dominated by the LAGEOS measurements.

The translation and rotation parameters of the Helmert transformation are on the same order of magnitude as in the reference solution and result within the formal errors each week.

The order of magnitude of the scale remains unaffected by swapping 20% of the NPs from LAGEOS to Etalon compared to the reference scenario. This implies that no significant translation or rotation is introduced by replacing 20% of LAGEOS observations with Etalon observations. We can see the maximum values of the parameters in Fig. 17 occur in the same weeks as in Fig. 6. Stations that did not observe in the reference scenario since the stations contributing observations to the solution remain the same.

Next the effect of the increased number of NPs to Etalon on the coordinates for two stations (station 7090 Yarragadee and 7237 Changchun) is analyzed in detail. Figures 18 and 19 compare the residuals of the weekly Helmert transformation for the reference scenario, the scenario with a 20% reduction of LAGEOS NPs and the scenario with increased Etalon observations. We observe very similar values in all components for all three scenarios.

A similar behavior can be seen for the station 7237 Changchun in Fig. 19. The Changchun station only obtains 30% of the number of LAGEOS observations compared to Yarragadee, and therefore also only the same fraction of Etalon NPs in the scenario with an increased amount of Etalon observations. Nevertheless the difference is within 4 mm if the two outliers in North and East component in, respectively, the first and third week of the year with values of 35 mm in North and 15 mm in East are ignored. The same weeks also stand out for the station 7090. In these weeks, only very few stations delivered NPs and a considerable fraction of NPs were provided by stations that usually do not observe Etalon very well. This leads to a larger Etalon-specific noise and a larger impact of the change in observations. In a perfect real case scenario it might be necessary to have reach a determined minimal number of NPs for LAGEOS before tracking Etalon with a higher priority instead of a totally homogeneous tracking ratio between weeks with high and low overall tracking coverage.

This is remarkable for two reasons, although the NPs to Etalon that replace 20% of the NPs to LAGEOS have a larger simulated noise, the solution of the station coordinates is not influenced in a negative way and further, Yarragadee provides the largest number of NPs; therefore, it has the largest number of reduced NPs to LAGEOS and the most added NPs to Etalon and thus the largest impact on the station coordinates can be expected. The station coordinates of the increased Etalon scenario remain within less than ± 2.5 mm of the ones in the reference scenario. The largest differences, and also a larger scatter, occur among stations that did not observe Etalon at all in the reference scenario. Thus, it can

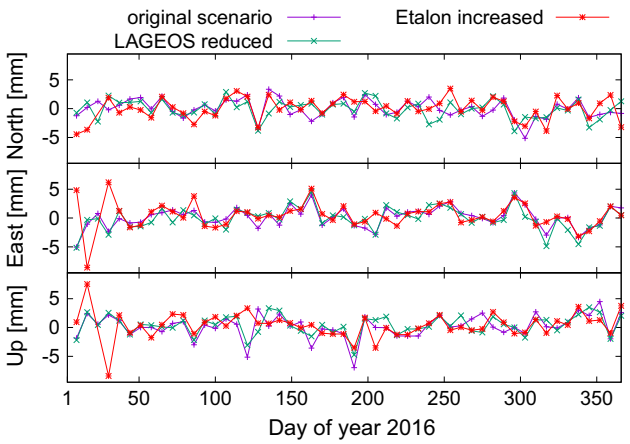

Fig. 18 Residuals of the Helmert transformation in local System for station 7090 (Yarragadee)

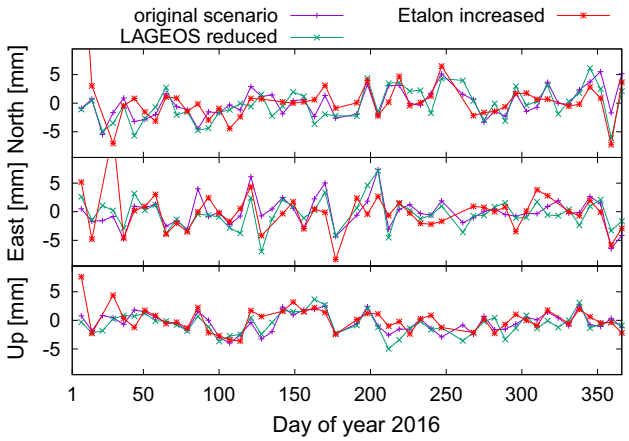

Fig. 19 Residuals of the Helmert transformation in local System for station 7237 (Changchun)

be concluded the station coordinates remain within the limits of Table 1 if 20% of NPs to LAGEOS are replaced by NPs to Etalon.

The most significant improvement gained by having more Etalon observations at hand can be seen in the recovery of the ERPs estimated in the solution. In Fig. 20, the differences between the ERPs derived from the increased Etalon scenario and the ERPs used for the simulation and second between the ERPs of the reference scenario without any reduction and the same ERPs that were used for the simulation of the NPs are shown. We can observe that this difference is roughly 9% smaller over all parameters for the 20% increased Etalon scenario. This is due to LAGEOS and Etalon having very different orbital characteristics, and considerably more stations providing Etalon NPs at all.

Having a larger number of 30% compared to only 10% of Etalon observations in the weekly ILRS standard solution and the same number of stations observing LAGEOS and Etalon in the estimation of the ERPs each week therefore proves again to be beneficial (Fig. 20). Although the a posteriori RMS increased by 5% due to the higher noise of the Etalon observations, the formal errors of the ERPs are slightly smaller in the scenario with an increased quantity of Etalon measurements (Fig. 21).

The cofactor matrix is the inversion of the normal equation and is influenced by the observation geometry and indicate the formal errors of the parameters. The elements of the cofactor matrix scale with the a posteriori RMS, which is slightly higher when a larger number of comparably noisier NPs is used in the processing. This is the case in the increased Etalon tracking scenario and nevertheless results in smaller formal errors. This means that the effect of the altered geometric distribution of the observations is more significant than the larger errors of Etalon NPs and stabilizes the solution leading to a better recovery of the ERPs.

Compared to the simulation reference scenario (Fig. 9), the differences between the LAGEOS orbits used for the simulation and the ones estimated from the simulated NPs remain at the 100 mm level for all three components (Fig. 22), whereas for Etalon the orbits improved from differences between ± 300 mm previously to differences within ± 200 mm in the worst cases in all three components (Fig. 23). This means more accurate orbits for Etalon can be obtained without degrading the LAGEOS orbits.

The differences of the obtained geocenter coordinates and the ones of the reference solution without reduction are within 5 mm in all weeks, meaning that the additional Etalon NPs did not influence the geocenter coordinates significantly.

Overall, it was demonstrated that the station coordinates and Helmert parameters remain at a similar level to the reference solution, even after replacing 20% of NPs to LAGEOS by NPs to Etalon, with their higher noise level for all stations. Having this increased amount of Etalon observations improved the recovery of the ERPs.

6 System bias

Thus far, only a higher realistic noise for Etalon NPs was considered. Now, by adding a separate systematic bias, further different systematic errors of SLR observations unique to Etalon as a target compared to LAGEOS, and their effects on the parameters of the solution can be simulated.

In order to use realistic values for this purpose, the station specific range bias estimations for LAGEOS and Etalon as provided by the data quality control at Deutsches Geodätisches Forschungsinstitut (DGFI) at the Technical University of Munich (DGFI 2016) have been used.

These biases vary from week to week for each station and may reach in the worst case a maximum of up to a cou-

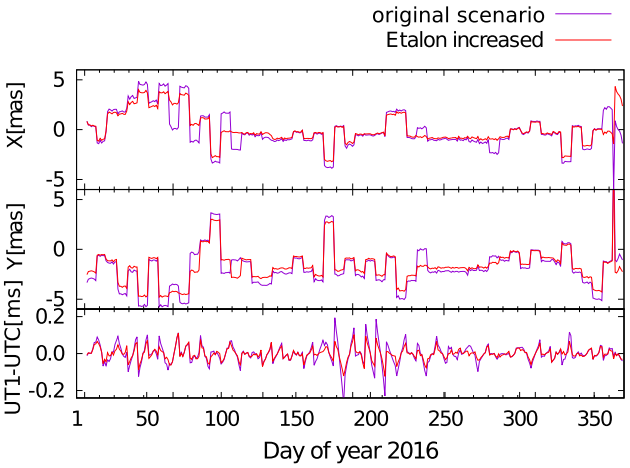

Fig. 20 Comparison of the ERP recovery for the reference scenario and the scenario with an increased amount of Etalon measurements

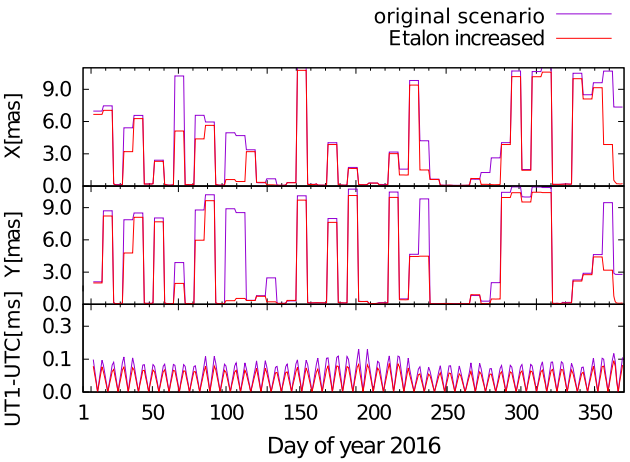

Fig. 21 Comparison of the formal errors of the ERPs for the reference scenario and the scenario with an increased amount of Etalon measurements

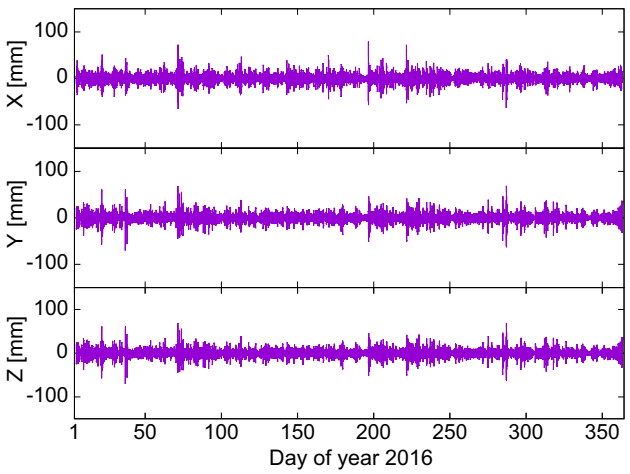

Fig. 22 Differences in LAGEOS estimated orbits between the reference solution and simulation in Earth-fixed system

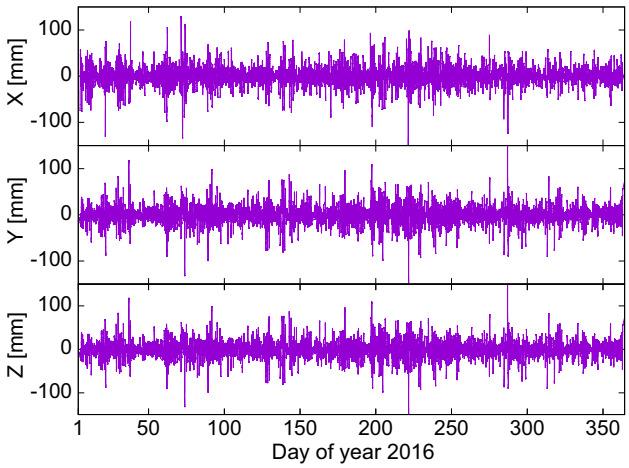

Fig. 23 Differences in Etalon estimated orbits between the reference solution and simulation in Earth-fixed system

ple of centimeters for individual stations in certain weeks. LAGEOS biases for the majority of stations are typically around 15 mm with standard deviation of 5 mm with the best stations only showing a bias of a few millimeters. Meanwhile, Etalon range biases are typically larger for most stations on a level of 60 mm with a standard deviation of 15 mm.

Using the range biases estimated by the DGFI for LAGEOS and Etalon for each station, their difference was added to all simulated NPs to Etalon as a weekly station specific system bias difference to simulate such a systematic error of SLR observations among different targets. Therefore, in addition to the pseudorandom noise (Eq. 1), the bias b_i is added to the exact distance of all Etalon NPs for each station i in addition to the pseudorandom noise. This effectively results in a shift of the simulated noise curve for each station i (as shown in Fig. 3) by b_i for all Etalon observations.

The question is whether the benefits of having more Etalon NPs in the weekly solution, as discussed in Sect. 5, would be diminished by such a bias. The most significant impact of this bias can be expected when a large number of Etalon observations are present. Thus, the tracking scenario with 20% reduced NPs to LAGEOS and an increase of NPs to Etalon by the number of reduced LAGEOS NPs was analyzed directly.

For this purpose, the parameters of the Helmert transformation between the station coordinates used for the simulation and the coordinates resulting from the simulated NPs including the bias are compared. The RMS values of the Helmert transformation increase by up to such that the mean value of the difference in RMS between the station coordinates used for the simulation and the solution for the scenario with an increased amount of Etalon measurements

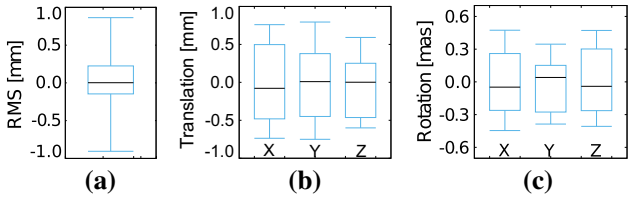

Fig. 24 Box plot of the difference in parameters of the Helmert transformation between the solution with increased number of NPs to Etalon and the scenario with an increased amount of Etalon measurements including a weekly station specific system bias for Etalon. **a** RMS; **b** translation parameters; **c** rotation parameters

including Etalon specific range biases is now 0.9 mm, compared to 0.5 mm as shown in Fig. 16 without the added bias. Additionally, the RMS values show a slightly larger scatter compared to the ones in the previous section. The distribution of the differences in RMS values between the solution with increased number of NPs to Etalon and the scenario with an increased amount of Etalon measurements including a weekly station specific system bias is given in Fig. 24a.

Figure 24b, c show box plots of the differences in translation and rotation parameters of the Helmert transformation between the solution with increased number of NPs to Etalon and the scenario with an increased amount of Etalon measurements including a weekly station specific system bias. The effect of this added bias on the rotation and translation parameters of the Helmert transformation was not significant in any of the three components. The values of the translation parameters were within less than 1 mm of the results without the added bias (Fig. 17), with formal errors increased by only 3%. The rotation parameters (Fig. 24c) also remain within a fraction of the formal error at the same values than in the solution without bias.

The scale, equivalently, is not significantly affected. Therefore, the effect of this bias on the station coordinates is only very minor for two reasons. In general, there are still more than twice as many NPs available for LAGEOS than Etalon, and the stations with the largest output tend to have small weekly range biases on the level of 10–20 mm compared to other stations with larger biases. Thus, the comparably small number of Etalon NPs with a larger bias does not destabilize the solution to a significant extent. In the past, i.e., the data of the year this study is based on, biases were not yet estimated on a weekly basis by the ILRS analysis centers. This will change with freely adjusted weekly biases estimated for each station and satellite pair in the future.

Last, and most importantly an improvement in the recovery of the ERPs can still be observed as seen in the previous section. When a bias is introduced, however, this improvement decreases slightly to 7% (Fig. 25), compared to 9% over all parameters (Fig. 20).

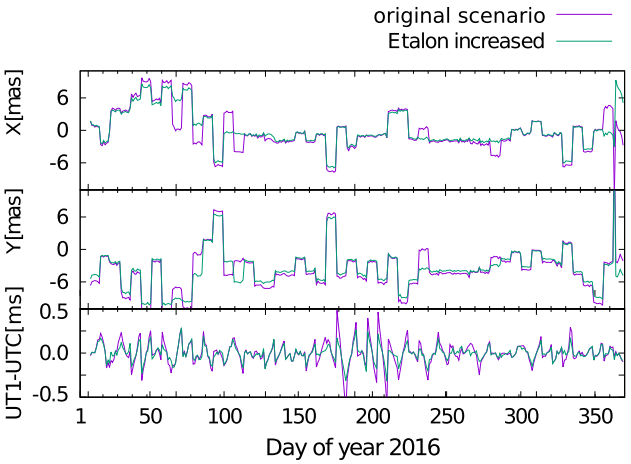

Fig. 25 Comparison of the ERP recovery for the reference scenario and the scenario with an increased amount of Etalon measurements including a weekly station specific bias for Etalon

Finally, when estimating the range bias while calculating the solution[1] for the scenario with 20% of LAGEOS NPs replaced by Etalon NPs, the priory introduced biases can be recovered on a level of less than 3 mm. In this case, the resulting solution is almost indistinguishable from the equivalent solution without a bias. An increased amount of Etalon NPs however improves the estimation of bias parameters for Etalon.

In summary, the introduced bias for Etalon observations only shows small effects on the station coordinates and Helmert parameters, which lie far below the established threshold given in Table 1.

The ERPs are still recovered better than in the reference tracking scenario. The quality of the Etalon orbits decreased slightly from roughly 100–120 mm maximum differences.

7 Conclusions

The solutions computed from these synthetic NPs compare well to the solution that was used to simulate the NPs in the case of a one-to-one replacement. We were able to distinguish between the effect that different initial seeds for the pseudorandom noise algorithm and the overall distribution of the observations have on the parameters of the solution. The specific availability of observing stations and the amount of NPs provided by each one had a larger influence than the variation of the seed of the random number algorithm.

In this simulation environment it is possible to reduce the observations to LAGEOS by 20% and retain the same level of quality in the estimated parameters of the ILRS weekly

[1] Which is what will be done by the ILRS moving forward.

standard solution for station coordinates, ERPs, and satellite orbits. The reduction up to this point proved to remain within the boundaries set by the effect threshold defined by the effect of the observation geometry. Therefore, this represents a possibility to gain additional tracking capability which can be used for other less intensively observed satellites, without expanding the current station network or the specific operating and tracking capabilities of the stations.

Keeping the same number of NPs in the combined weekly LAGEOS and Etalon solution but shifting up to 20% of the LAGEOS tracking volume toward the Etalon satellites does not affect most of the parameters of the solution. The orbits of the Etalon satellites, as expected, improve when tripling the number of NPs in a given week from up to 300 mm to only 100 mm maximum differences in an Earth-fixed reference frame. Most importantly, the ERPs used for simulating the NPs can be recovered better by almost 10% when having higher contributions from Etalon observations in the combined solution.

The simulation takes into account different noise levels for LAGEOS and Etalon. Additionally, different weekly station specific effects between SLR observations to LAGEOS and Etalon can be studied by adding range biases in the simulation. When adding such an additional range bias of magnitudes as estimated by DGFI (2016) to the Etalon observations, it is still possible to have an improved solution in the case of 20% of LAGEOS NPs replaced by Etalon NPs. The Helmert parameters and ERPs got slightly worse, although not significantly. The ERP parameters were still recovered better by an average of 7% over all three components.

The improvement of certain parameters as presented in this study serves as an example of possible benefits from an altered tracking strategy. With the quickly increasing number of satellites that are equipped with laser retroreflectors, i.e., GNSS satellites, the current station network can not keep up its current performance over a larger number of targets. Building new stations or updating existing ones to a point where the performance is up to the level of the most productive stations should be pursued with available resources. In the meantime, however, it will be viable to use the existing tracking capability of the network in an optimized way. Reducing the observations to the two LAGEOS satellites, which are among the highest tracked targets, results in a relatively large amount of potential NPs that can be used to support the ever extending list of targets.

Acknowledgements This research project was funded by the Swiss National Science Foundation (SNSF) Grant *200020_157062 Swiss Optical Ground Station and Geodynamics Observatory Zimmerwald* and relied on the excellent work of the (Pearlman et al. 2002, ILRS) managing, supporting and supplying the SLR data products.

References

Altamimi Z, Rebischung P, Mativier L, Xavier C (2016) ITRF2014: a new release of the International Terrestrial Reference Frame modeling nonlinear station motions. J Geophys Res Solid Earth. https://doi.org/10.1002/2016JB013098

Andritsch F, Grahsl A, Dach R, Jäggi A (2016) Simulation of realistic SLR observations to optimize tracking scenarios. In: Proceedings of the 20th International Workshop on Laser Ranging, 10–14 October 2016, Potsdam, Germany

Appleby G, Rodríguez J, Altamimi Z (2016) Assessment of the accuracy of global geodetic satellite laser ranging observations and estimated impact on ITRF scale: estimation of systematic errors in LAGEOS observations 1993–2014. J Geod. https://doi.org/10.1007/s00190-016-0929-2

Bizouard C, Gambis D (2012) The combined solution C04 for Earth Orientation parameters consistent with International Terrestrial Reference Frame 2008. Observatoire de Paris, Paris, France

Dach R, Lutz S, Walser P, Fridez P (eds) (2015) Bernese GNSS Software Version 5.2. User manual. University of Bern, Bern Open Publishing, Astronomical Institute. ISBN 978-3-906813-05-9. https://doi.org/10.7892/boris.72297

DGFI (2016) Recent results from SLR data quality control. http://ilrs.dgfi.tum.de/quality/weekly_biases/. Accessed May 2017

James F (1994) RANLUX—a FORTRAN implementation of the high-quality pseudrandom number generator of Luscher. Comput Phys Commun 79(1):111–114

Kehm A, Bloßfeld M, Pavlis E, Seitz F (2018) Future global SLR network evolution and its impact on the terrestrial reference frame. J Geod. https://doi.org/10.1007/s00190-017-1083-1

Knuth D (1997) The art of computer programming, volume 2: seminumerical algorithms, 3rd edn. Section 3.2.1: the linear congruential method. Addison-Wesley, Boston, pp 10–26. ISBN 0-201-89684-2

Marsaglia G, Bray T (1964) A convenient method for generating normal variables. SIAM Rev 6(3):260–264

Matsumoto M, Nishimura T (1998) Mersenne twister: a 623-dimensionally equidistributed uniform pseudorandom number generator. ACM Trans Model Comput Simul 8:3–30

Nishimura T (2000) Tables of 64-bit Mersenne twisters. ACM Trans Model Comput Simul 10:348–357

Noll C, Pearlman M, Torrence M (2015) Summary of results from ILRS GNSS tracking campaigns (2014–2015). In: Presented at the, (2015) ILRS Technical Workshop, 24–30 October 2015. Matera, Italy

Otsubo T, Matsuo K, Aoyama Y et al (2016) Effective expansion of satellite laser ranging network to improve global geodetic parameters. Earth Planets Space. https://doi.org/10.1186/s40623-016-0447-8

Pavlis E, Kuzmicz-Cieslak M (2008) SLR and the next generation global geodetic networks of low satellites. In: Schilliak S (ed) The 16th International Workshop on Laser Ranging, 13–17 October 2008. Poznan, Poland

Pearlman M, Degnan J, Bosworth J (2002) The international laser ranging service. Adv Space Res 30(2):135–143

Pearlman M, Bianco G, Merkowitz S, Noll C, Pavlis E, Shargorodsky V, Zhongping Z (2016) ILRS: current status and future challenges. In: Presented at the Fall American Geophysical Union meeting, 06–12 December, San Francisco, CA, USA

Ricklefs R, Moore C (2009) Consolidated laser ranging data format (CRD), version 1.01, October 27 2009. https://ilrs.cddis.eosdis.nasa.gov/docs/2009/crd_v1.01.pdf. Accessed May 2017

Sinclair A, The International Laser Ranging Service (1997) Data screening and normal point formation: re-statement of Herstmonceux normal point recommendation, June 1997. https://ilrs.cddis.eosdis.nasa.gov/data_and_products/data/npt/npt_algorithm.html. Accessed June 2017

Thaller D, Sośnica K, Dach R, Jäggi A, Beutler G (2011) LAGEOS-ETALON solutions using the Bernese Software. In: Mitteilungen des Bundesamtes für Kartographie und Geodäsie Band 48. Proceedings of the 17th International Workshop on Laser Ranging, 16–20 May 2011. Bad Kötzting, Germany